EUROPEAN ORGANIZATION FOR NUCLEAR RESEARCH
ORGANISATION EUROPEENNE POUR LA RECHERCHE NUCLEAIRE

CERN - PS DIVISION

PS/ CA/ Note 99-14
SL Note 99-32 (MD)

MISMATCH MEASUREMENT AND CORRECTION TOOLS FOR THE PS-SPS TRANSFER OF THE 26 GEV/C LHC BEAM

G. Arduini, J. Colchester, G. Ferioli, M. Giovannozzi, J-J. Gras, K. Hanke,
D.J. Hopkins, R. Jung, D. Manglunki, M. Martini

Abstract

Transverse emittance preservation is a major concern for the LHC injector chain. Minimisation of the blow-up due to mismatch at injection into the SPS is therefore mandatory. While the transverse position of the beam in the SPS injection line is monitored bunch-by-bunch by an Optical Transition Radiation (OTR) screen and a fast detector, the phase space matching at injection is monitored by an OTR based mismatch monitor in the SPS ring. Orthogonal tuning knobs were developed to tune independently Twiss parameters, dispersion and dispersion derivative. In this paper, we describe the mismatch correction mechanism as well as the two monitoring systems. We report on first measurements which were carried out during the 1998 SPS run and on the improvements that we intend to pursue during the 1999 run.

Geneva, Switzerland
28 July 1999

SL-Note-99-032 MD
PS-Note-99-014 CA

PS/SPS

Mismatch Measurement and Correction Tools for the PS-SPS Transfer of the 26 GeV/c LHC Beam

July 28, 1999

G. Arduini, R. Colchester, G. Ferioli, M. Giovannozzi, J.-J. Gras, K. Hanke, D. J. Hopkins, R. Jung, D. Manglunki, M. Martini

Keywords: PS Machine, SPS Machine, Optics, LHC Injector Chain

Run no.	Date
	05/12/98

Summary

Transverse emittance preservation is a major concern for the LHC injector chain. Minimisation of the blow-up due to mismatch at injection into the SPS is therefore mandatory. While the transverse position of the beam in the SPS injection line is monitored bunch-by-bunch by an Optical Transition Radiation (OTR) screen and a fast detector, the phase space matching at injection is monitored by an OTR based mismatch monitor in the SPS ring. Orthogonal tuning knobs were developed to tune independently Twiss parameters, dispersion and dispersion derivative. In this paper, we describe the mismatch correction mechanism as well as the two monitoring systems. We report on first measurements which were carried out during the 1998 SPS run and on the improvements that we intend to pursue during the 1999 run.

1 Introduction

The TT2/TT10 transfer line between the PS and the SPS machines will be an important part of the LHC injector chain [1]. In order to optimise beam transport and emittance preservation, the beam line must be matched accurately to the nominal lattice functions at the SPS injection point given the measured optical functions at the PS extraction point. In order to quantify the quality of the matching, we define the geometrical betatronic mismatch factor as

$$G_b = H + \sqrt{H^2 - 1}, \tag{1}$$

where

$$H = \frac{1}{2}\left[\frac{\beta_0}{\beta_m} + \left(\alpha_0 - \alpha_m\frac{\beta_0}{\beta_m}\right)^2\frac{\beta_m}{\beta_0} + \frac{\beta_m}{\beta_0}\right]. \tag{2}$$

The emittance blow-up after filamentation is then given by

$$\varepsilon_{\text{after fil.}} = \varepsilon_0 H. \tag{3}$$

In the previous equations α_m, β_m stand for the measured Twiss parameters while α_0, β_0 are the nominal Twiss parameters. The transfer line optics was modelled and re-matched for the 26 GeV/c LHC beam

during the 1998 SPS run. For the matched optics, we found a betatron mismatch after filamentation of 1.0 in both planes. This clearly fulfils the LHC requirements. The dispersion mismatch after filamentation was computed to 1.7 in the horizontal and 1.0 in the vertical plane [2]. The residual mismatch is both due to the unavoidable discrepancy between model and real machine and to the uncertainty in the measurement of the initial beam parameters.

2 Orthogonal Knobs

Given the unavoidable residual mismatch, it is mandatory to tune selected beam parameters without changing the global setting of the line. There are eight beam parameters to be corrected: the horizontal and vertical α-parameter, the horizontal and vertical β-function as well as the horizontal and vertical dispersion and dispersion derivative. In order to control these quantities independently, eight free parameters are required. The matching section of the TT10 line consists of 10 quadrupoles. Since two pairs of them are powered in series, this setup provides exactly the eight required degrees of freedom. The rest of the TT10 line, which represents the SPS lattice, as well as the TT2 quadrupoles were not used in a first approach for simplicity considerations in the control of these elements.

2.1 Analytical Approach

The change in the optical parameters due to the variation of the eight independent quadrupole strength parameters can be described by a set of eight equations of the type

$$\Delta\alpha_H = \frac{\partial\alpha_H}{\partial K_1^{(1)}}\Delta K_1^{(1)} + \frac{\partial\alpha_H}{\partial K_1^{(2)}}\Delta K_1^{(2)} + \cdots + \frac{\partial\alpha_H}{\partial K_1^{(8)}}\Delta K_1^{(8)} + O[(\Delta K_1^{(n)})^2], \tag{4}$$

where $\Delta K_1^{(n)}$ is the variation of the strength parameter of the n^{th} quadrupole. Taking into account only the linear terms, the formalism can be generalised introducing an 8×8 matrix $\mathbf{M}$ whose coefficients are given by the variation of the beam parameters per unit change of quadrupole strength:

$$\begin{bmatrix} \Delta\alpha_H \\ \Delta\beta_H \\ \Delta D_H \\ \Delta D'_H \\ \Delta\alpha_V \\ \Delta\beta_V \\ \Delta D_V \\ \Delta D'_V \end{bmatrix} = \begin{bmatrix} \frac{\partial\alpha_H}{\partial K_1^{(1)}} & \frac{\partial\alpha_H}{\partial K_1^{(2)}} & \cdots & \cdots & \frac{\partial\alpha_H}{\partial K_1^{(8)}} \\ \frac{\partial\beta_H}{\partial K_1^{(1)}} & \cdots & \cdots & \cdots & \cdots \\ \vdots & \cdots & \cdots & \cdots & \vdots \\ \vdots & \cdots & \cdots & \cdots & \vdots \\ \frac{\partial D'_V}{\partial K_1^{(1)}} & \cdots & \cdots & \cdots & \frac{\partial D'_V}{\partial K_1^{(8)}} \end{bmatrix} \begin{bmatrix} \Delta K_1^{(1)} \\ \Delta K_1^{(2)} \\ \Delta K_1^{(3)} \\ \Delta K_1^{(4)} \\ \Delta K_1^{(5)} \\ \Delta K_1^{(6)} \\ \Delta K_1^{(7)} \\ \Delta K_1^{(8)} \end{bmatrix} \tag{5}$$

The vector on the right-hand side is given by the variation of the quadrupole strength, the vector on the left gives the resulting change in the beam parameters. The units follow the notation used in *MAD* [3]: α [1], β [m], D [m], D' [1], K_1 [m^{-2}]. The eight strength parameters refer to the following magnets in the matching section of TT10:

$K_1^{(1)}$:	QIID1001	$K_1^{(5)}$:	QID1005
$K_1^{(2)}$:	QIIF1002	$K_1^{(6)}$:	QIF1006
$K_1^{(3)}$:	QIID1003	$K_1^{(7)}$:	QID1007 & QID1009
$K_1^{(4)}$:	QIF1004	$K_1^{(8)}$:	QIF1008 & QIF1010.

The 64 coefficients of the matrix are obtained from a *MAD* simulation of the transfer line: the strength of the relevant quadrupoles is varied one at a time by a certain amount and the variation of the beam parameters at the injection point is recorded. This procedure yields the required coefficients.
If the matrix is not singular, it can be inverted and the required variation of the quadrupole strengths for a given change in any of the beam parameters directly be computed. For instance, a change of D_H by -0.1 m while leaving all other beam parameters unchanged would be described by

$$\begin{bmatrix} \Delta K_1^{(1)} \\ \vdots \\ \vdots \\ \Delta K_1^{(8)} \end{bmatrix} = \mathbf{M}^{-1} \begin{bmatrix} 0 \\ 0 \\ -0.1 \\ 0 \\ \vdots \\ 0 \end{bmatrix}$$

If the matrix is not singular, it can be inverted and the required changes of the quadrupole strengths can be directly computed.

2.2 Numerical Algorithm

Frequently, as in our case, the matrix M of a given optics is either singular or numerically close to singular. The physical reason for this is that one quadrupole (or combination of quadrupoles) may be very efficient to tune a given beam parameter while another combination may be completely inefficient. Singular Value Decomposition (SVD) algorithms provide a tool to diagnose a matrix and to solve systems of equations of the form

$$\mathbf{M} \cdot \mathbf{x} = \mathbf{b} \tag{6}$$

such as (5) even for ill-conditioned matrices [4].

SVD algorithms are based on the theorem, that any $m \times n$ ($m \geq n$) matrix can be written as a product of three matrices,

$$\mathbf{M} = \mathbf{U} \cdot \mathbf{S} \cdot \mathbf{V}^t, \tag{7}$$

where **S** is a diagonal matrix whose elements are referred to as the singular values of **M**:

$$\mathbf{S} = [diag(w_j)]. \tag{8}$$

If **M** is, as in our case, a square matrix, **U**, **V** and **S** have the same size. The matrices **U** and **V** are orthogonal, that is $U^{-1} = U^t$ and similarly for V. Hence, inverting (7) yields

$$\mathbf{M}^{-1} = \mathbf{V} \cdot [diag\left(\frac{1}{w_j}\right)] \cdot \mathbf{U}^t. \tag{9}$$

The elements of **S** allow to diagnose the matrix **M**: if one ore more of the w_j have very small values which are beyond the computation precision, the matrix is numerically singular. It can be re-conditioned by setting the corresponding $(1/w_j)$ in $\mathbf{S}^{-1}$ to zero. Having done this, the system of equations can be solved as

$$\mathbf{x} = \mathbf{V} \cdot [diag\left(\frac{1}{w_j}\right)] \cdot (\mathbf{U}^t \cdot \mathbf{b}). \tag{10}$$

The solution vector x will not be the exact solution but the best possible one in a least square sense. The physical interpretation is, that a large eigenvalue corresponds to an efficient quadrupole combination while a small eigenvalue corresponds to an inefficient one. In fact, looking at the eigenvalues sorted by SVD, one will find in general a smooth decay from large (efficient combinations) to small (inefficient combinations) values, and a step down to values close to zero. These singularities correspond to combinations which are completely useless and should be set to zero in the inverted matrix.

3 Transverse Position Monitoring

The results obtained for the transverse beam parameters are relying on a precise measurement of the beam profile and therefore on the absence of badly kicked bunches. A monitor was installed in the TT10 injection line to measure the transverse position of every single bunch during injection. The measurement station (Fig. 1) uses a standard BTV SPS tank, where an OTR radiator is placed at 45° with respect to the beam. The radiation passes through a window and a set of neutral density filters and is then focused by a $f = 75$ mm lens onto a Multi-anode Photo Multiplier Tube (MPMT). This MPMT preserves the spatial distribution of intensity between photo cathode and anode. It has 16 anodes measuring 0.8×16 mm with a 1 mm pitch and an anode pulse rise time of about 0.6 ns. A motorised rotation stage can rotate the MPMT from 0° to 90°, which allows to take both horizontal and vertical profiles with the same monitor. The set of filters, the gain of the MPMT and the rotation stage are remotely controlled. The 16 anodes are acquired simultaneously at a rate of 40 MHz. The measurements showed that the first bunch in the batch was horizontally off-centred by 5 mm and had a lower intensity (Fig. 2). Attempts were made by the PS to adjust the extraction kicker timing during the MD.

4 Injection Mismatch Monitoring

4.1 SPS Matching Monitor

Successful tuning of beam parameters at injection into the SPS requires the ability to monitor on-line the effect on the injected beam. For the 1997 run, a dedicated monitor was installed in LSS4 with optimised OTR light collection for the low injection energy, i.e. wide opening angle $1/\gamma$. A thin 12 μm titanium foil is placed at 45° with respect to the beam trajectory and the backward optical transition radiation is collected. This system provides an imaging of the injected 26 GeV/c proton beam for about 130 revolutions, after which the beam suffers from significant blow-up. It was shown that the beam can be left circulating with the target in place for more than 300 turns without damaging the foil. The set-up is shown schematically in Fig. 3.

The transition radiation is sampled by a pulsed intensifier and acquired on a CCD used as a fast buffer memory to acquire successive turns of the beam. A measurement result is shown in Fig. 4. It shows a very clean signal, with only a few noise peaks on the whole CCD surface and a slope of thermal origin which can be subtracted during the processing. At the beginning of the measurement sequence, a reference image is taken before the first injection. This reference image will be subtracted from the following measurements, suppressing the thermal slope as well as inhomogeneities due to dark current. The horizontal and vertical projections are obtained from the individual beam images, from which the beam sizes are calculated with a Gaussian fit using a χ^2 minimisation routine.

The main limitation in the image acquisition rate was found to be the acceptable repetition rate of the intensifier. The rate, and hence the image acquisition, could be increased to 10 kHz only by using a high strip current MCP intensifier. To have some safety margin, the acquisition rate was decreased to one out of eight SPS turns, i.e. 5.62 kHz, still much higher than the usual 25 Hz rate of normal frame grabbers. To fill in the data of the missing turns, a timing sequencer scans automatically the missing turns by displacing the first acquired turn for subsequent injections. A full profile history over 32 revolutions reconstructed with 8 successively injected pulses takes less than three minutes. This procedure relies on the stability of the beam.

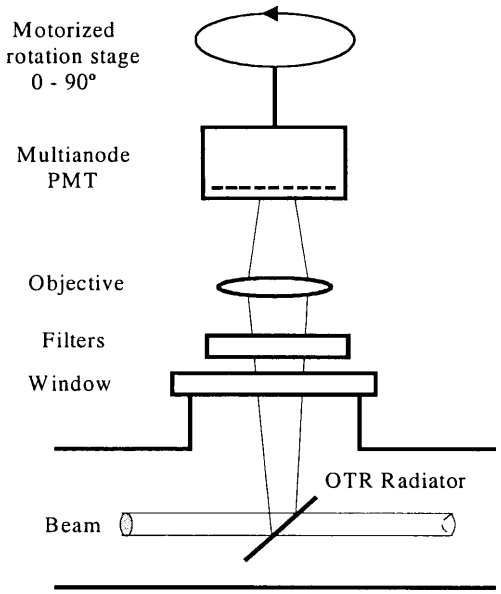

Figure 1: Schematic set-up of the bunch-by-bunch OTR monitor in TT10.

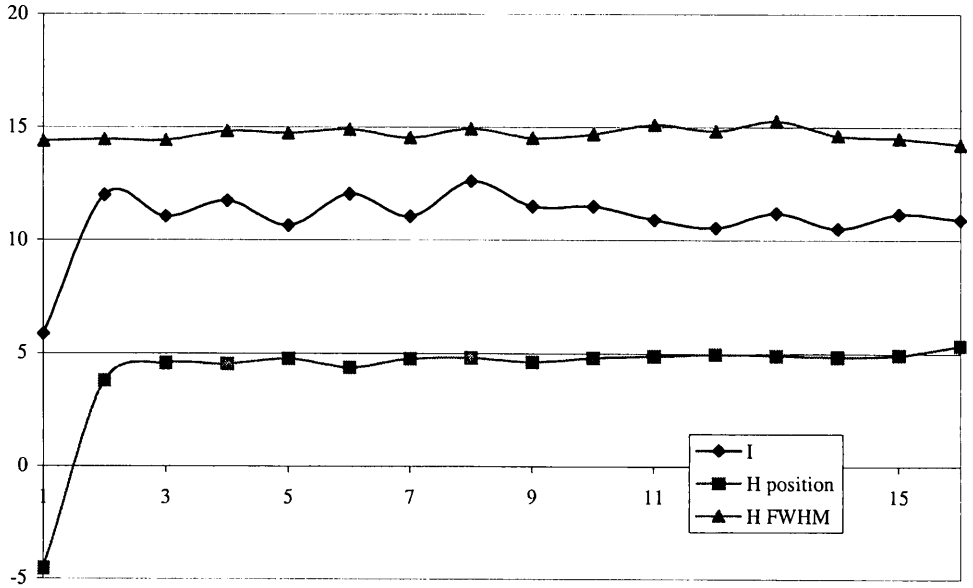

Figure 2: Intensity [a.u.], horizontal position [mm] and beam size [mm] of the 16 bunches of an injection measured with the fast profile monitor.

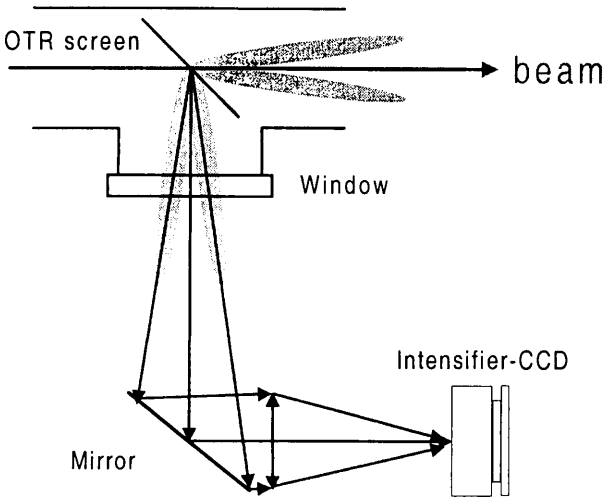

Figure 3: Schematic set-up of the OTR matching monitor in the SPS.

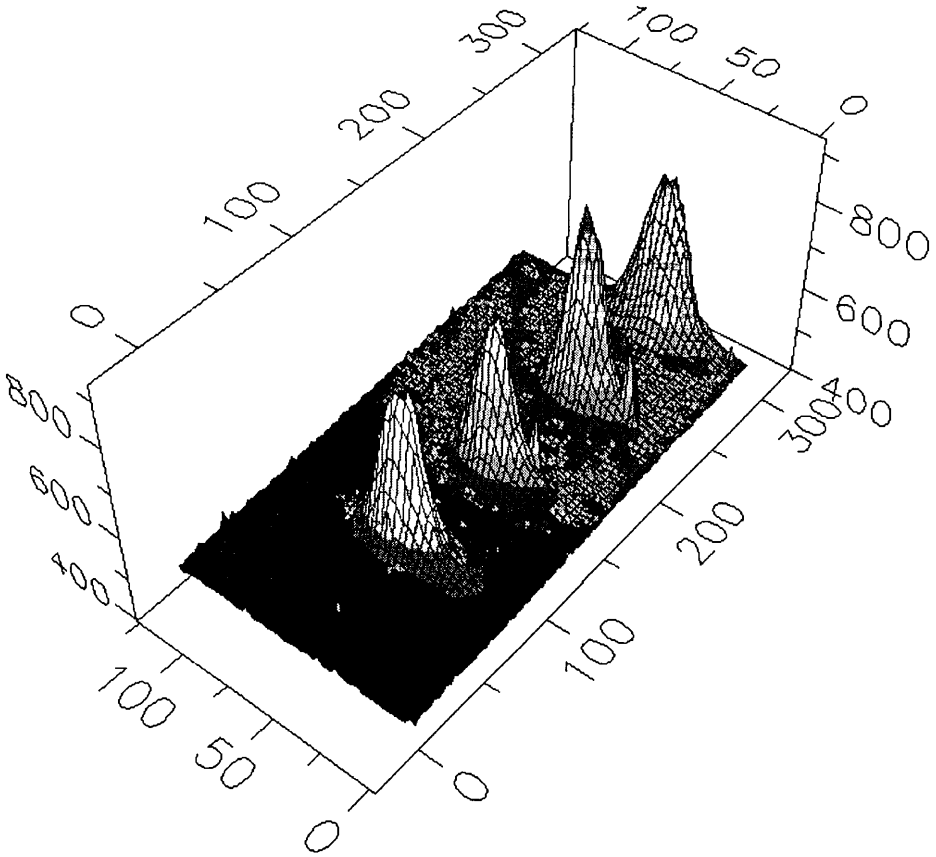

Figure 4: Result of the digitisation of four beam profiles from different SPS turns memorised on the CCD. The beam dimensions are given in pixels [500 μm/px] and the amplitude in counts of the 12 bit ADC.

4.2 Experimental Results

The tuning tool described in Section 2 was experimentally tested, using the SPS mismatch monitor described in the previous section to observe the effect on the injected beam. While the oscillation of the beam size indicates mismatch, it is important to obtain also the numerical values of the beam parameters at the injection point in order to compute the required correction. Starting from a matched setting, the horizontal and vertical β-functions were detuned and the beam parameters at the injection point monitored using the SPS mismatch monitor. Table 1 shows the beam parameters at the injection point into the SPS for the matched transfer line optics. Starting from this setting, β_H and β_V were

	Horizontal plane	Vertical plane
β [m]	102.01	20.75
α	-2.33	$5.55 \cdot 10^{-1}$
D [m]	$5.30 \cdot 10^{-2}$	$5.31 \cdot 10^{-2}$
D'	$5.65 \cdot 10^{-3}$	$-5.33 \cdot 10^{-3}$

Table 1: Nominal optical parameters at the injection of the TT2/TT10 line into the SPS for matched optics as computed with *MAD*.

detuned by $\pm 10\%$ and $\pm 20\%$.

4.2.1 Analysis of Three Turns

The Twiss parameters can be obtained from a measurement of the beam profile at three successive turns in the SPS. They are then computed in the same way as from the standard three-grid measurement in a transfer line assuming that the dispersion function is known. This is in fact the case, since the dispersion for the first turn in the SPS has been measured for this optics [2]. The values of the dispersion function at the location of the monitor can therefore be obtained from a simulation for any turn in the machine. Figure 5 shows the measured horizontal β-function at the injection point versus the variation of β_H applied using the tuning knob. The expected change of β_H (dashed line) obtained using the matrix of Eq. (5), the result obtained from the simulation and the measured values are shown. It can be seen, that already in the simulation the expected variation is not achieved. As far as the measurement is concerned, only the points for $\Delta\beta = 0$, -10 m and -20 m could be measured due to a technical problem. The measurement suffers from significant fluctuations in the horizontal plane which do not allow to draw any conclusion. The vertical β-function for the same measurement is shown in Fig. 6. Simulated and measured results remain unchanged as specified.

Figures 7 and 8 show the horizontal and vertical α-parameter for the same measurement. Within the error in both planes the measured results agree with the expected ones.

From the measured Twiss parameters, the mismatch factor can be computed. Figure 9 shows the horizontal mismatch factor versus change of β_H for the same measurement. The large fluctuations in the horizontal plane make a conclusion impossible. The vertical mismatch factor is shown in Fig. 10. A slight variation is observed.

The same measurement was done in the vertical plane. Figure 11 shows theoretical, simulated and measured values of β_V for five different settings of the tuning knob. All values agree within the statistical error. From the same measurement the horizontal β-function was determined. The result is shown in Fig. 12. The value of β_H remains unaffected by the variation of β_V within the error.

Figures 13 and 14 show the vertical and horizontal α-parameter for the same measurement. Both remain unchanged as specified.

From the Twiss parameters, again the geometrical mismatch factors in both planes were computed. The results are shown in Figs. 15 and 16. In both cases the mismatch factor shows the expected behaviour: the vertical mismatch has its minimum approximately for the matched optics ($\Delta\beta_V = 0$). Detuning β_V in both directions increases the vertical mismatch as specified. The horizontal mismatch factor is not affected by the variation in the vertical plane. Note, however, the significant error on this measurement.

As a general remark, we would like to stress the point that in the horizontal plane the imposed variation of β-function is not a linear function of $\Delta\beta_H$. Therefore, the linear model described by Eq. (5) gives only a poor approximation of the actual variation of Twiss parameters due to the influence of the neglected high order terms.

5 Error Considerations

The error bars in Figs. 5 - 16 represent the standard deviation obtained from the analysis of several sets of data. Besides this statistical error, some systematic error sources can be identified.

As mentioned in Section 3.2, it was observed that the bunches at the edge of the batch can be off-centred. Since these bunches will oscillate around the position of the other bunches at the betatron frequency, they will induce spurious beam size oscillations. This could explain the problems encountered with the measurements in the horizontal plane as the extraction from the PS is performed horizontally.

The three-grid method is based on the knowledge of D, D', $\Delta p/p$ as well as of the single turn transfer matrix at the monitor position. The transfer matrix is normally well known as the strength of the quadrupoles and of the bending dipoles is precisely measured. D and D' should be measured at least in one point of the injection line at any stage of the tuning procedure. This could only be done once before starting the experiment.

5.1 Coulomb Scattering and Energy Loss in Foil

The beam suffers from blow-up due to Coulomb scattering when passing through the OTR foil. The measured beam size shows therefore not only an oscillation due to the mismatch, but also a positive slope which is due to the crossing of the foil. The blow-up due to Coulomb scattering was experimentally computed to be 35 μm per passage. The measured beam size has to be corrected for this. Figure 17 shows the evolution of the uncorrected measured beam size. The oscillation and the positive slope can be clearly seen.

In addition, the protons loose a fraction of their energy when passing through the OTR screen. For a thin target (smaller than the radiation length), the energy deposit in [MeV] per particle and per passage can be parametrised as

$$\Delta E = 1.5[\mathrm{MeVcm^2g^{-1}}]l[\mathrm{cm}]\rho[\mathrm{gcm^{-3}}], \tag{11}$$

where the first factor is due to ionisation losses, l is the thickness of the target and ρ is the density of the target material. In our case (12 μm Ti) this yields an energy loss of 8.1×10^{-3}MeV per turn and per particle. The presence of horizontal dispersion at the monitor couples the longitudinal and transverse planes. The energy loss in the monitor will therefore induce an emittance blow-up in the horizontal plane. The emittance growth (per turn) due to the energy loss is given by

$$\frac{\Delta\varepsilon}{\varepsilon} = \frac{1}{\varepsilon}\left(\beta D'^2 + 2\alpha DD' + \gamma D^2\right)\left(\frac{\Delta E}{E}\right)^2,$$

which yields $\frac{\Delta\varepsilon_H}{\varepsilon_H} = 2 \times 10^{-9}$ which is negligible.

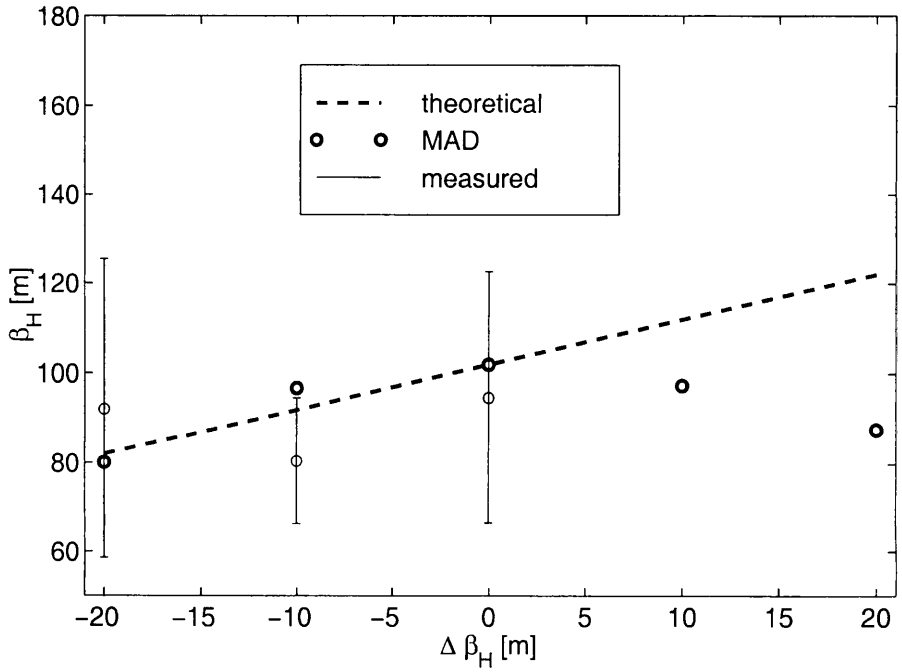

Figure 5: Horizontal β-function at the TT10 injection point versus variation of β_H applied using the tuning knob. Starting from a matched optics ($\Delta\beta_H = 0$), the horizontal β-function is decreased by 10 m and 20 m. The simulation does not follow the theoretical curve for $\Delta\beta_H$ = +10 m and +20 m.

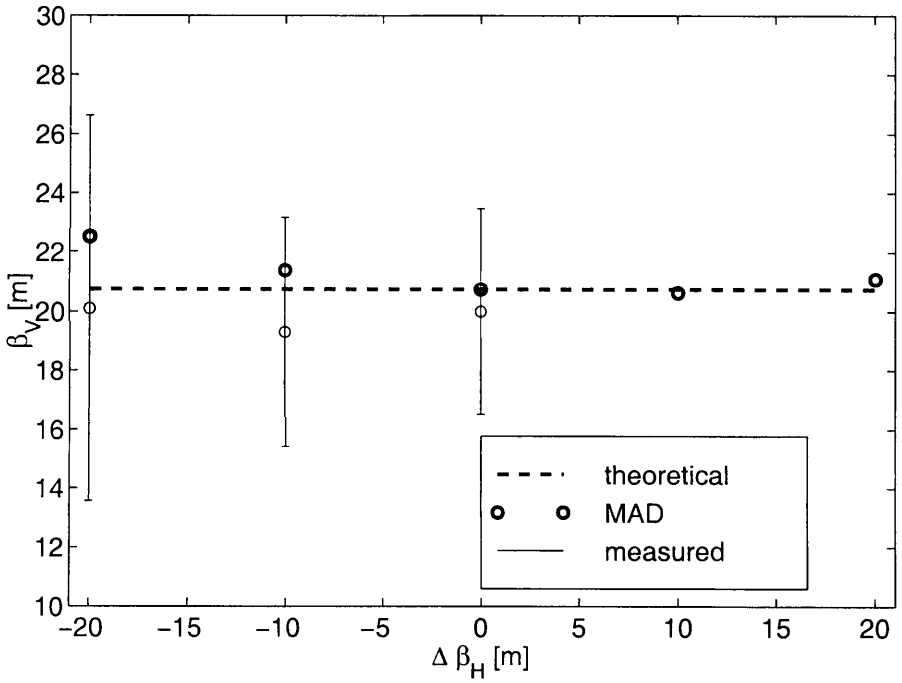

Figure 6: Vertical β-function for the same measurement: β_V stays constant as specified.

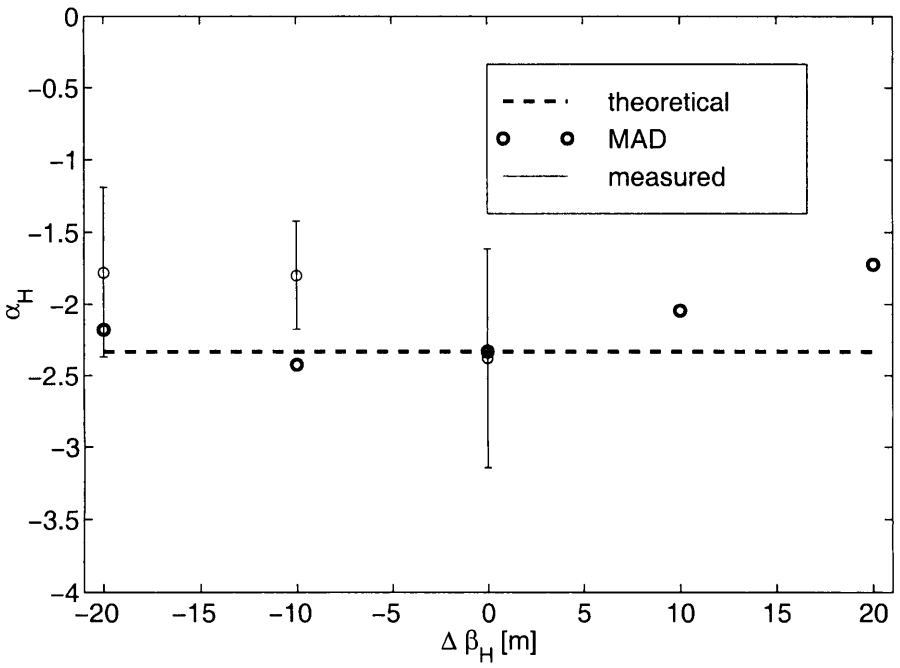

Figure 7: Horizontal α-parameter at the TT10 injection point versus variation of β_H: α_H stays constant within the measurement error.

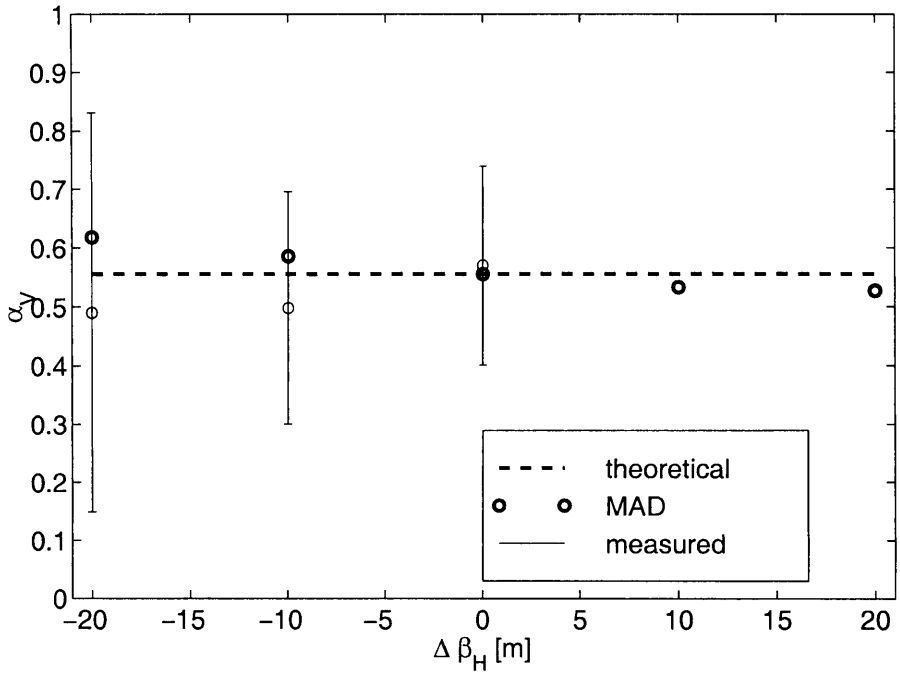

Figure 8: Vertical α-parameter for the same measurement: α_V stays constant as specified.

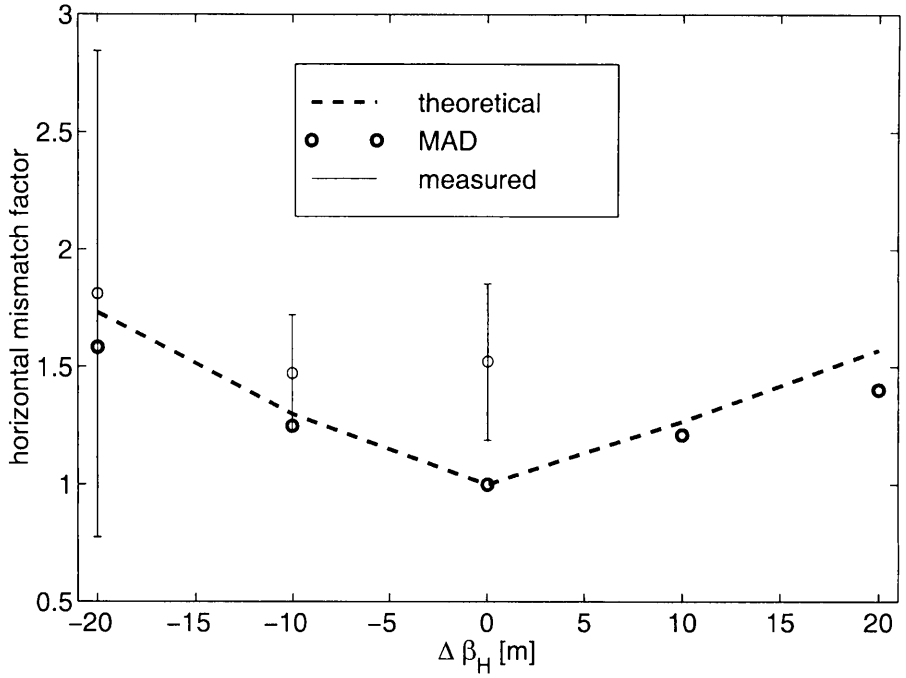

Figure 9: Horizontal geometrical mismatch factor at the TT10 injection point versus variation of β_H. The measurement suffers from large fluctuations in the horizontal plane.

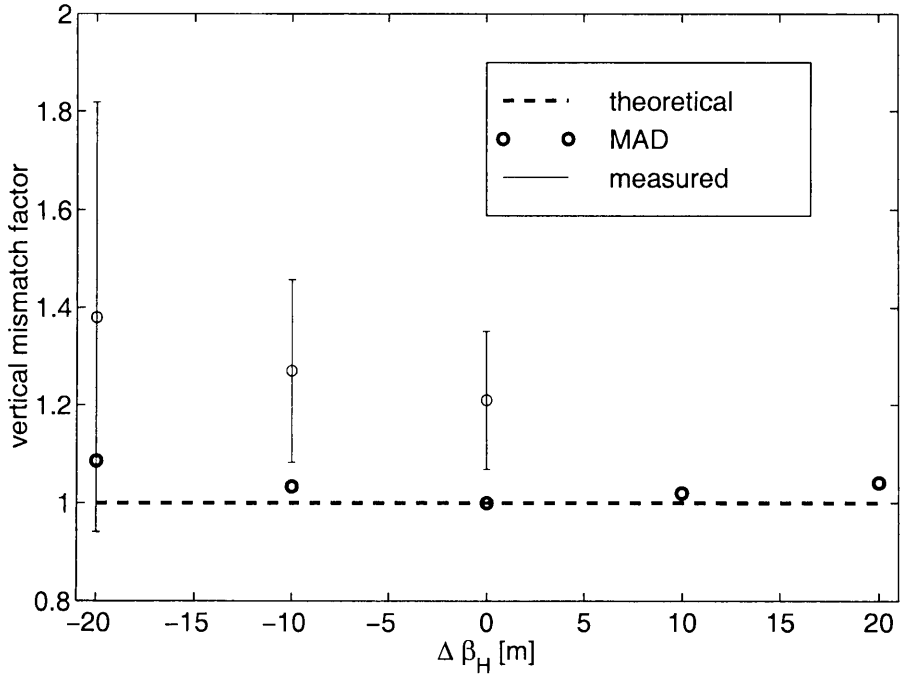

Figure 10: Vertical geometrical mismatch factor for the same measurement. Only a slight variation is observed.

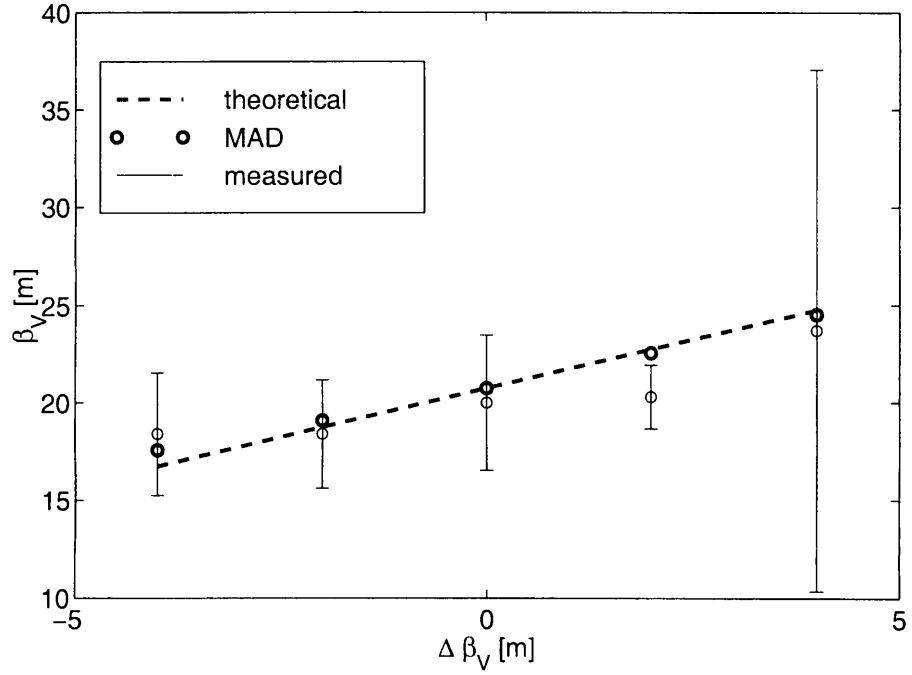

Figure 11: Vertical β-function at the TT10 injection point versus variation of β_V applied using the tuning knob. Starting from a matched optics ($\Delta\beta_V = 0$), the vertical β-function is increased and decreased by 2 m and 4 m.

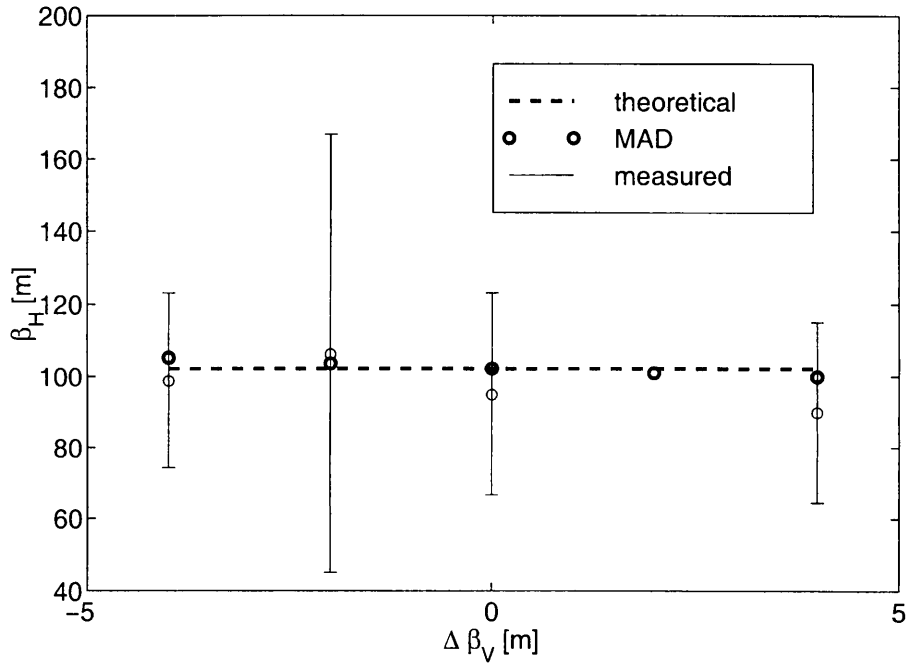

Figure 12: Horizontal β-function for the same measurement: β_H stays constant as specified.

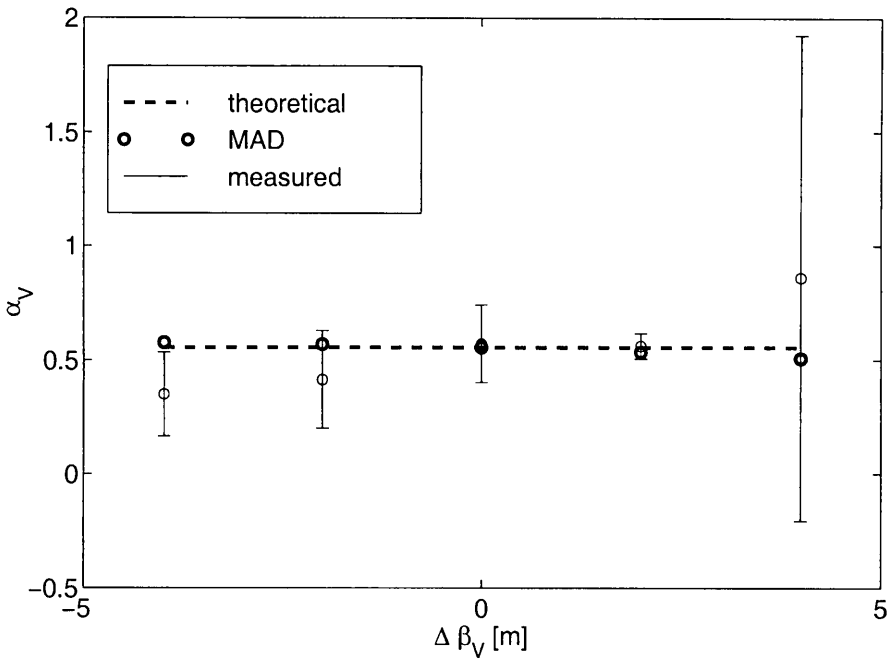

Figure 13: Vertical α-parameter at the TT10 injection point versus variation of β_V: α_V stays constant as specified.

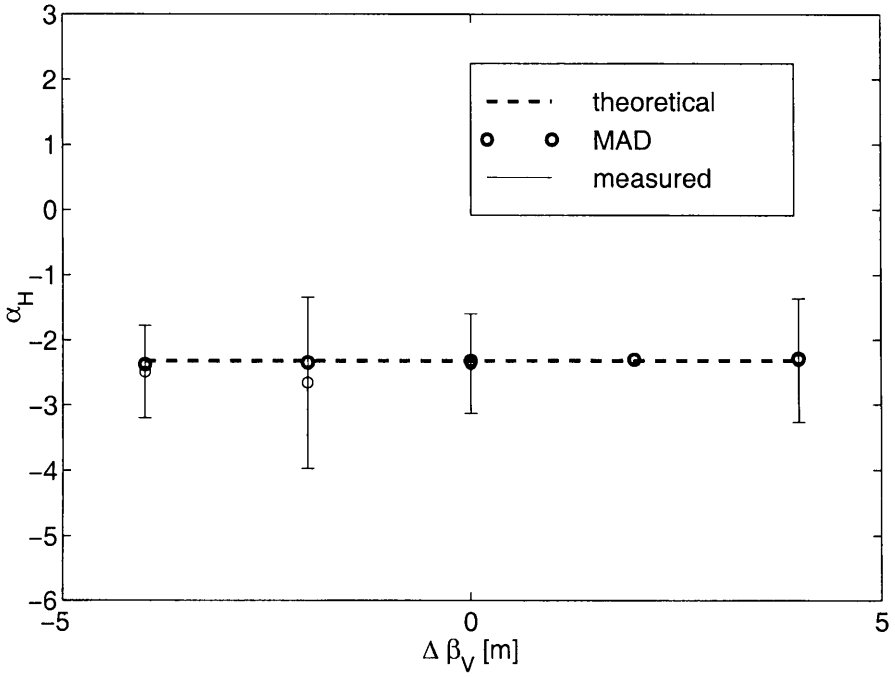

Figure 14: Horizontal α-parameter at the TT10 injection point for the same measurement: α_H stays constant as specified.

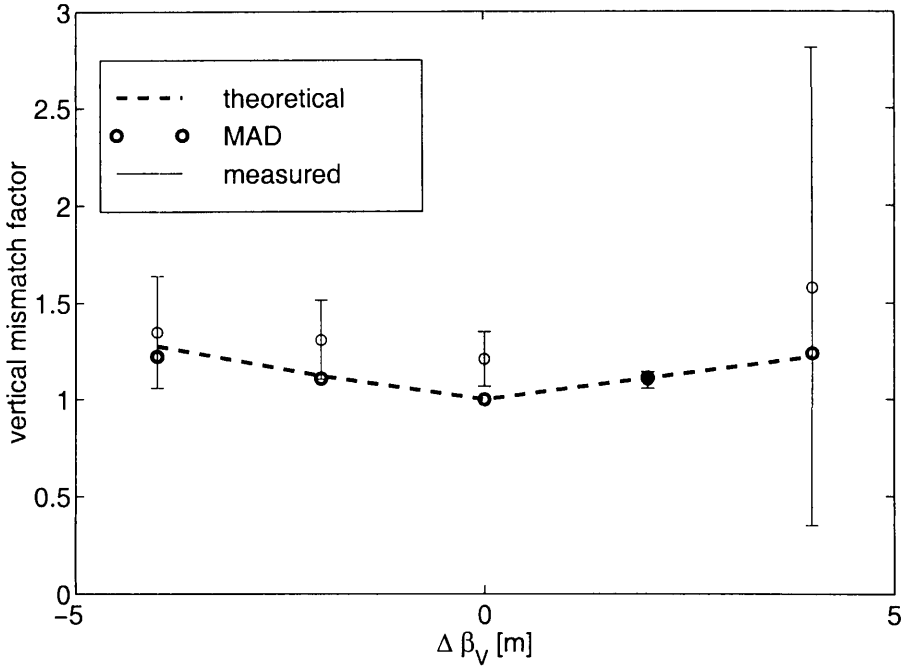

Figure 15: Vertical mismatch factor versus variation of β_V. Starting from a matched optics, detuning of β_V leads to an increase of the vertical mismatch as specified.

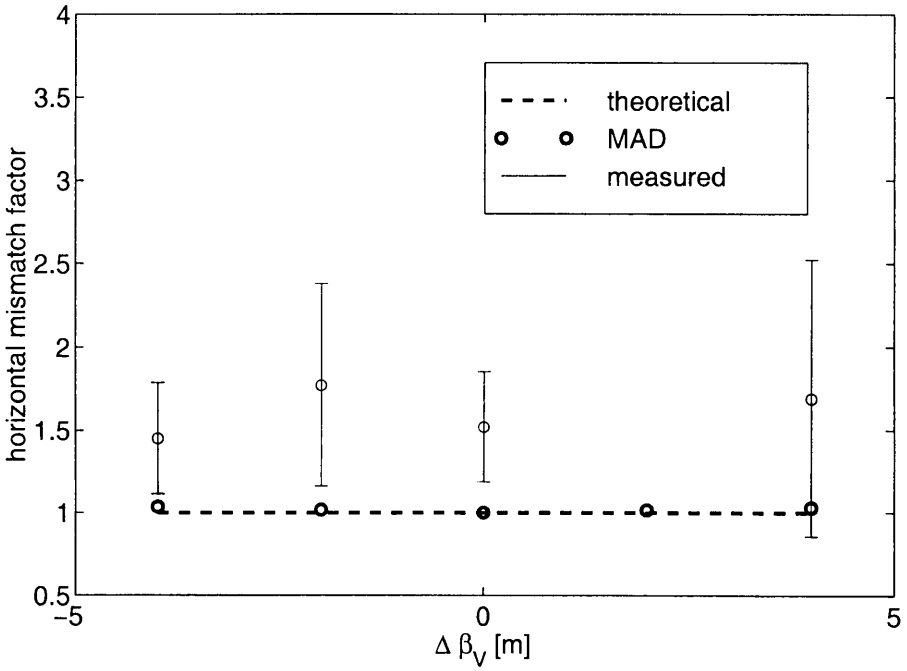

Figure 16: Horizontal mismatch factor for the same measurement. The horizontal mismatch stays constant within the error.

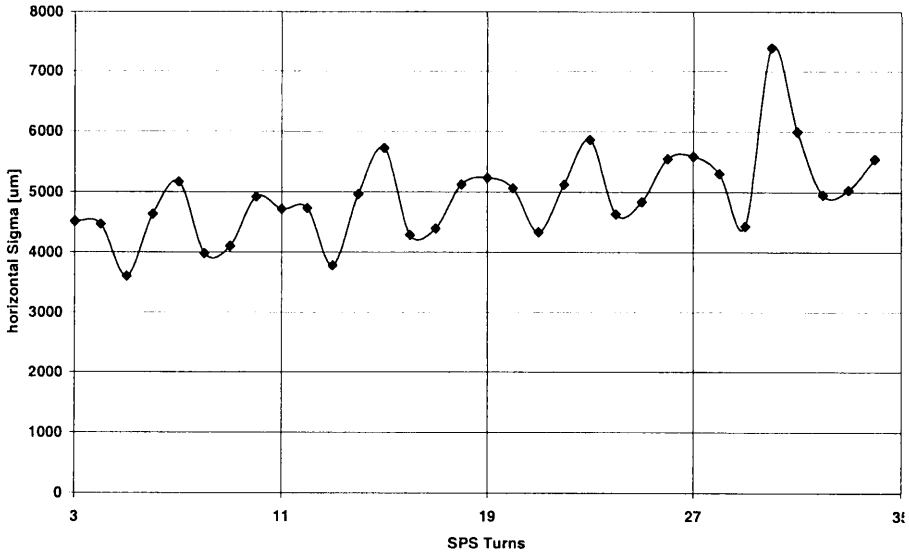

Figure 17: Uncorrected measured horizontal beam size versus number of turns in the SPS. The oscillations indicates mismatch, the positive slope blow-up due to the foil.

6 Conclusion and Outlook

A straight-forward analytical approach was used to develop a tool for selective tuning of beam parameters in the PS-SPS transfer line. Eight independent quadrupole strengths provide the necessary degrees of freedom to tune eight beam parameters. A coefficient matrix which contains the dependence of the optical parameters on the eight quadrupole strengths was generated based on a *MAD* simulation of the line. It was then re-conditioned and inverted using an SVD algorithm. The resulting system of equations can be solved and yields the change of quadrupole strength required to obtain a given change of any of the Twiss parameters.

A *MAD* simulation showed that the tuning knob works fine for all beam parameters except the horizontal β-function. A first measurement with beam, carried out during the 1998 SPS run, gave the expected results in the vertical plane. In the horizontal plane the results suffer from significant fluctuations.

It is planned to improve the tuning knob by using more magnets as degrees of freedom. In a first step, the quadrupoles in the TT2 part of the line will be used. If this does not lead to the required improvement, the installation of new hardware will be considered.

The analysis of the output of the mismatch monitor, presently done off-line, will be implemented such that quantitative values of the optical parameters at the TT10 injection point are provided on-line. This can, in turn, be used as input to compute the quadrupole setting required for the mismatch correction. To this aim we are investigating the possibility of using the new multi-profile method [5] already applied in the TT2/TT10 transfer line. This new approach allows to simultaneously measure the Twiss parameters, beam emittance, dispersion function and its derivative without changing any beam parameter (as it is done in the standard way of measuring the dispersion function). This would allow to verify the effect of the tuning knob on D and D' and the elimination of a systematic uncertitude on the measurement of the Twiss parameters. This will require the acquisition of at least 5 profiles per injection.

Dispersion matching is also desirable before starting the measurement in order to minimise the uncertainty on the Twiss parameter measurements.

Acknowledgements

The authors would like to thank R. W. Assmann and P. Raimondi for fruitful discussions. We would furthermore like to thank the PS and SPS operation teams for their support.

References

[1] P. Collier (ed.), *The SPS as Injector for LHC, Conceptual Design*, CERN-SL-97-07 DI (1997).

[2] G. Arduini, M. Giovannozzi, K. Hanke, D. Manglunki, G. Métral, *Betatron and Dispersion Matching of the TT2/TT10 Transfer Line for the LHC Beam*, CERN PS-Note-99-007 CA and CERN SL-Note-99-003 MD (1999).

[3] H. Grote, F. C. Iselin, *The MAD Program, User's Reference Manual*, CERN SL 90-13 AP (1990).

[4] B. P. Flannery, W. H. Press, S. A. Teukolsky, W. T. Vetterling, *Numerical Recipes in Fortran, The Art of Scientific Computing*, 2^{nd} edition, Cambridge University Press (1986).

[5] G. Arduini, M. Giovannozzi, D. Manglunki, M. Martini, *Measurement of the Optical Parameters of a Transfer Line using Multi-profile Analysis*, CERN PS 98-032 (CA) (1998).

Distribution List

R. Cappi	PS/CA
M. Giovannozzi	PS/CA
J-Y. Hémery	PS/CA
D. Manglunki	PS/CA
M. Martini	PS/CA
G. Métral	PS/OP
J-P. Riunaud	PS/CA
K. Schindl	PS/DI